Published in final edited form as:
Cell Signal. 2018 May 01; 45: 132–144. doi:10.1016/j.cellsig.2018.01.026.

New insights into the Vav1 activation cycle in lymphocytes

María Barreira[a,b], **Sonia Rodríguez-Fdez**[a,b], **Xosé R. Bustelo**[a,b,c,*]

[a]Centro de Investigación del Cáncer, Consejo Superior de Investigaciones Científicas (CSIC), University of Salamanca, 37007 Salamanca, Spain

[b]Instituto de Biología Molecular y Celular del Cáncer, Consejo Superior de Investigaciones Científicas (CSIC), University of Salamanca, 37007 Salamanca, Spain

[c]Centro de Investigación Biomédica en Red de Cáncer (CIBERONC), Consejo Superior de Investigaciones Científicas (CSIC), University of Salamanca, 37007 Salamanca, Spain

Abstract

Vav1 is a hematopoietic-specific Rho GDP/GTP exchange factor and signaling adaptor. Although these activities are known to be stimulated by direct Vav1 phosphorylation, little information still exists regarding the regulatory layers that influence the overall Vav1 activation cycle. Using a collection of cell models and activation-mimetic Vav1 mutants, we show here that the dephosphorylated state of Vav1 in nonstimulated T cells requires the presence of a noncatalytic, phospholipase Cγ1–Slp76-mediated inhibitory pathway. Upon T cell stimulation, Vav1 becomes rapidly phosphorylated via the engagement of Lck and, to a much lesser extent, other Src family kinases and Zap70. In this process, Lck, Zap70 and the adaptor protein Lat contribute differently to the dynamics and amplitude of the Vav1 phosphorylated pool. Consistent with a multiphosphosite activation mechanism, the optimal stimulation of Vav1 can only be recapitulated by the combination of several activation-mimetic phosphosite mutants. The analysis of these mutants has also unveiled the presence of different Vav1 signaling competent states that are influenced by phosphosites present in the N- and C-terminal domains of the protein.

Keywords

Exchange factors; Rac1; JNK; NFAT; Lck; Src family; Zap70; Lat; Phospholipase Cγ; Slp76; Protein tyrosine phosphatases; T cell receptor; B cell receptor; Phosphosites; Conformational states; Signaling diversification; Lymphocytes

*Corresponding author at:Centro de Investigación del Cáncer, Consejo Superior de Investigaciones Científicas (CSIC), University of Salamanca, 37007 Salamanca, Spain, xbustelo@usal.es (X.R. Bustelo).

Author contributions

M.B. and S.R-F. carried out the experiments, analyzed the data generated, and contributed to artwork design. X.R.B. conceived the work, analyzed data, wrote the manuscript, and carried out the final editing of figures.

Competing interests

The authors report no competing financial interests.

Europe PMC Funders Author Manuscripts

1 Introduction

Vav1 mainly works as a tyrosine phosphorylated-regulated Rho guanosine nucleotide exchange factor (GEF), a catalytic activity that allows the rapid transition of Rho GTPases from the inactive (GDP-bound) to the active, GTP-bound state during cell signaling [1,2]. In addition, it displays in some contexts adaptor functions that allow the regulation of downstream signals using catalysis-independent mechanisms [1,3]. For example, Vav1 can promote the Cbl-b-mediated degradation of the intracellular domain of Notch1 [4,5] and the Ca^{2+}-dependent stimulation of the nuclear factor of activated T-cells (NFAT) [6–9], a transcriptional factor essential for the expression of cytokines and other activation-connected proteins in lymphocytes [10]. These adaptor functions can be dependent (NFAT) or independent (Notch1) of the phosphorylation state of Vav1 [1,3–5].

Vav1 is characterized by a multidomain structure that harbors calponin homology (CH), acidic (Ac), Dbl homology (DH), pleckstrin homology (PH), C1-subtype zinc finger (C1), proline-rich (PRR), SH3, and SH2 regions [1] (Fig. 1A). These domains play roles related to the intramolecular regulation of the protein (CH, Ac, PH, SH3) [1,11–14], the activation step (SH2, SH3) [15–17], the catalytic process (DH, PH, C1) [13,14,18,19], the establishment of interactions with protein partners (PRR, SH3, SH2), and the catalysis-independent regulation of NFAT (CH) and Notch1 (the two SH3s) [1,6,8,9,14,20–22]. Whereas the basis of the regulation of the catalytic activity of Vav proteins is well characterized at the structural level [18,19], the mechanism of stimulation of the NFAT route by Vav1 is still poorly understood. However, it is known that it involves the stimulation of phospholipase Cγ (PLCγ) which, upon the IP_3-mediated mobilization of Ca^{2+} from intracellular stores, favors the stimulation of the phosphatase calcineurin by Ca^{2+}-calmodulin [9]. This phosphatase promotes in turn the dephosphorylation of cytoplasmic NFAT and its final shuttling to the nucleus (Fig. 1B). Unlike the case of the catalysis-dependent pathways, the NFAT route requires the parallel action of Vav1 and other TCR-stimulated signaling pathways to achieve full activation in cells [6] (Fig. 1B). As a result, this pathway can be further stimulated by the TCR even when cells express constitutively active Vav1 proteins (e.g., $Vav1^{\Delta 835–845}$) [23]. Also in contrast to the catalysis-dependent pathways, the NFAT route cannot be activated by constitutively active Vav1 proteins lacking the CH domain (e.g., $Vav1^{\Delta 1–66}$, Vav $1^{\Delta 1–144}$, $Vav1^{\Delta 1–184}$) (Fig. 1B) [1,6,8,9,14,20,21].

The inactive state of Vav proteins is maintained by inhibitory intramolecular interactions established by the CH, Ac and most C-terminal SH3 (CSH3) regions with the catalytic DH-PH-C1 core (Fig. 1A) [12,23]. This “closed” structure shifts towards an “open” conformation upon the phosphorylation of tyrosine residues located in the Ac (Y^{142}, Y^{160}, Y^{174}), CSH3 (Y^{836}) and, to a lesser extent the C1 region (Y^{541}, Y^{544}) [21,23] (Figs. 1A and S1). Consistent with this model, mutations that eliminate the foregoing inhibitory structure lead to the generation of phosphorylation-independent, constitutively active proteins [1,13,14,24]. This activation can be unexpectedly achieved using both Tyr to Glu and Tyr to Phe mutations [12,14,21,23], an effect probably due to the implication of the side chains of these phosphosites in the stabilization of the intramolecular inhibitory structure [11,12]. In the case of antigen receptors, the Vav1 activation step requires the stepwise action of adaptors and PTKs that, in many cases, are cell type-specific. For

example, in T cells, this step entails the membrane tethering of Vav1 by adaptor molecules (e.g., Grb2, Nck, Lat) and, subsequently, the ensuing phosphorylation by TCR-activated protein tyrosine kinases [1,25].

Despite these advances, there are still open questions associated with the mechanism of activation of Vav1 and rest of family members. For example, it is still unclear which PTK(s) phosphorylate them downstream of antigen receptors, as many kinases (Lck, Fyn, Hck, Syk) are capable of promoting both the phosphorylation and catalytic activation of Vav proteins in vitro [1,2,13,24]. The multiple phosphorylation sites involved in this activation step also pose the possibility that Vav proteins could adopt different conformational and signaling states depending upon the number of tyrosine residues phosphorylated at a given time on the molecule [23]. In line with this, we do not know whether the engagement of the catalytic and adaptor functions of these proteins is subjected to similar signaling constraints. We have addressed those issues in this work using a multifaceted approach based on the utilization of phosphosite-specific Vav1 antibodies, wild-type and mutant cell models, and activation-mimetic Vav1 phosphosite mutants. In addition, we used biological readouts that allowed us to monitor the catalytic and adaptor activities of Vav1 under each of the above experimental conditions.

2 Results

Lck is the main tyrosine kinase involved in optimal Vav1 activation in Jurkat cells.

We followed two intertwined approaches to assess the contribution of upstream PTKs to Vav1 signaling. On the one hand, we analyzed the phosphorylation status of endogenous Vav1 immunoprecipitated from parental, Zap70-deficient (P116 cell line) and Lck-deficient (J.Cam1.6 cell line) Jurkat cells [26,27] using immunoblots with antibodies to either general (pTyr) or specific Vav1 phosphorylated tyrosine residues (Y^{142}, Y^{160}, Y^{174}, Y^{836}; Fig. 1A). The specificity of these Vav1 phosphospecific antibodies was demonstrated in earlier studies [21,23]. On the other hand, we measured the effect of the loss of those PTKs on the activation of the catalytic activity of Vav1. To this end, we used a standard luciferase reporter assay to compare the stimulation of endogenous c-Jun N-terminal kinase (JNK) induced by the expression of a green fluorescent protein (EGFP)-tagged version of wild-type (WT) Vav1 in those cells. This assay is based in the ectopic expression of a fusion protein (encoded by the pFA2-cJun plasmid) composed of the c-Jun transcriptional activation domain and the DNA binding domain of the yeast GAL4 protein that, upon the phosphorylation of the c-Jun domain by endogenous JNK, promotes the expression of the *P. pyralis* luciferase from a second plasmid (pFR-Luc) that contains a synthetic promoter with 5 tandem repeats of the yeast GAL4 binding site (http://www.chem-agilent.com/pdf/strata/800050.pdf). Vav1 activates JNK in a Rac1-dependent manner and, therefore, the stimulation of this serine/threonine kinase can be used as a cell-based readout for the amount of Vav1 catalytic activity achieved in each experimental condition (Fig. 1B). Moreover, in this experimental context, the stimulation of JNK induced in Jurkat cells is strictly Vav1-dependent and, due to this, is not influenced by the engagement of other signaling pathways by the upstream TCR or the ancillary CD28 receptor. In addition to $Vav1^{WT}$, we utilized in some of these experiments a mutant version of Vav1 lacking the inhibitory

N-terminal domains ($Vav1^{\Delta 1–186}$) because, given its phosphorylation-independent catalytic activity [14,21,23,24], the evaluation of its activity allows for the direct assessment of the effect of the absence of PTKs under investigation on the engagement of downstream signaling pathways by activated Vav1 proteins.

We first tested the effect of the elimination of Zap70 on Vav1 phosphorylation using the P116 Jurkat cell line [26]. Previous results have shown that this cell line, although showing normal basal tyrosine phosphorylation levels, it cannot trigger optimal phosphorylation responses upon stimulation [26]. Consistent with this, we observed that the basal levels of phosphorylation of all the Vav1 phosphosites surveyed display no significant variations in this cell line when compared to control cells (Fig. 1C, left column of panels, compare 0 time points). However, against the canonical tyrosine kinase model for T cells, we found that the lack of Zap70 results in slight reductions in the total phosphorylation of Vav1 (Fig. 1C, left column, top panel) as well as in the phosphorylation of the Y^{142}, Y^{160} and Y^{174} phosphosites localized in the Vav1 Ac region (Fig. 1C, left column; second, third and fourth panels from top). These defects affect the amplitude rather than the kinetics of phosphorylation of all those residues (Fig. 1C, left column, four top panels). By contrast, the lack of Zap70 delays the phosphorylation kinetics of the Y^{836} residue located in the Vav1 CSH3 domain (Fig. 1C, left column, fifth panel from top). As we will show further below in this section, the phosphorylation of Vav1 under these conditions is under the control of Lck and, to a much lesser extent, other Src family kinases. Unlike the case of Vav1, we observed that the overall pattern of tyrosine phosphorylated proteins is severely affected by the lack of Zap70 in TCR-stimulated cells as previously described by others (Fig. S2A) [26].

The defective phosphorylation of Vav1 in Zap70-deficient cells does not seem important for its effective activation under optimal stimulation conditions, because $EGFP\text{-}Vav1^{WT}$ triggers similar amounts of JNK activity in both parental and Zap70 null cells (Fig. 1D, compare left and middle panels). The phosphorylation-independent, constitutively active version of Vav1 ($Vav1^{\Delta 1–186}$) can also stimulate JNK at similar levels in WT and Zap70-deficient cells (Fig. 1D, compare left and middle panels), further indicating that Zap70 is not required either for the effective signaling of active Vav1 proteins. As expected from its constitutive enzyme activity [14,23], this mutant version of Vav1 can stimulate JNK at high levels regardless of the stimulation state of the transfected cells (Fig. 1D, compare left and middle panels). We confirmed the appropriate expression of the EGFP and EGFP-Vav1 proteins in these experiments using Western blot analysis (Fig. 1E, left panel). The same technique was used to confirm the lack of Zap70 in the P116 Jurkat cell line utilized in these experiments (Fig. S2B).

In contrast to the foregoing results, we found using the Lck-deficient J.Cam1.6 cell line that the basal phosphorylation of Vav1 is severely affected in the absence of that kinase (Fig. 1C; middle column of panels, compare 0 time-points). In addition, the amplitude of the phosphorylation response of all the Vav1 phosphosites tested in TCR-stimulated J.Cam1.6 cells is severely reduced when compared to the WT counterparts (Fig. 1C, middle column, five top panels). The phosphorylation kinetics of the Y^{160}, Y^{174} and Y^{836} phosphosites are also delayed in the Lck-deficient cell line (Fig. 1C, middle column; third, fourth and fifth panels from top). As expected [27], the lack of Lck results in severe defects in both the

basal and TCR-dependent phosphorylation of most signaling proteins in Jurkat cells (Fig. S2A). The residual phosphorylation of Vav1 detected in TCR-stimulated J.Cam1.6 cells is probably mediated by the redundant function of other Src family kinases, as inferred from the total elimination of Vav1 phosphorylation upon the treatment of TCR-stimulated Lck null cells with a well-known Src family inhibitor (PP2) (Fig. 1C, middle column of panels). The same effect is observed when using TCR-stimulated J45.01 Jurkat cells lacking expression of CD45 [28] (Fig. 1C, right column of panels), the protein tyrosine phosphatase involved in the activation of Src family kinases in lymphocytes [25]. The reblotting of filters with antibodies to Vav1 confirmed that the changes in phosphorylation observed in all these experimental conditions are not due to variations in the amount of Vav1 immunoprecipitated from cells (Fig. 1C). These phosphorylation defects do affect the overall activation of Vav1, as demonstrated by the lack of activation of JNK when EGFP-Vav1^{WT} is expressed in Lck-deficient Jurkat cells (Fig. 1D, compare left and right panels). Lck is also partially required for the downstream signaling of active Vav1 proteins, as demonstrated by the mild, although statistically significant reduction in the activation of the JNK pathway when the constitutively active Vav1$^{\Delta 1-186}$ protein is expressed in J.Cam1.6 cells (Fig. 1D, compare the three panels). By contrast, J.Cam1.6 cells show levels of JNK activation similar to those found in the WT and P116 cell lines when the stimulation by the TCR is bypassed by the addition of phorbol 12-myristate 13-acetate (PMA) (Fig. 1D, bottom panels). The addition of an ionophore, either alone or in combination with PMA, does not induce any significant effect in this response (Fig. 1D, bottom panels). Immunoblot analyses confirmed the proper expression of the ectopic EGFP-fusion proteins used in these experiments (Fig. 1E, right panel). The expected absence of endogenous Lck and CD45 in the J.Cam1.6 and J45.01 cell lines was corroborated using immunoblot and flow cytometry determinations, respectively (Fig. S2C and S2D). Taken together, these data indicate that the phosphorylation of Vav1 in Jurkat cells does not follow the canonical TCR → Lck → Zap70 linear signaling cascade [25], relying instead on the convergent action of Lck, Zap70 and, to a lesser extent, other Src family kinases (Fig. 1F). There is a specialization in those kinases in this process, because Lck is important for ensuring the phosphorylation of all the phosphosites tested (Fig. 1F, step a) whereas Zap70 seems to be involved in the regulation of the overall amplitude of the phosphorylation of the tyrosine residues located in the Vav1 Ac domain as well as in the optimal kinetics of phosphorylation of the CSH3-located Y^{836} phosphosite (Fig. 1F, step b). In terms of biological activity, our results also indicate that Lck is the only kinase required to ensure the optimal activation and downstream signaling of Vav1 at least under conditions of ectopic overexpression. They also reveal that the Vav1 Ac and CSH3 phosphosites do not share a similar pattern of phosphorylation by upstream kinases.

2.1 Lat is important for Vav1 activation and downstream signaling

It has been shown before that Lat is important for Vav1 stimulation [1,29], although its impact on the phosphorylation of the key Vav1 regulatory phosphosites has not been assessed as yet. To tackle this issue, we compared the phosphorylation of endogenous Vav1 in control and Lat-deficient ANJ3 Jurkat cells [29]. The lack of this adaptor protein in the latter cells was confirmed by immunoblot analyses (Fig. 2A). The impact of this deficiency in the overall phosphorylation pattern of non-stimulated and TCR-stimulated cells was also determined using Western blot analyses with antibodies to pTyr residues (Fig.

S3, left panel). We found that the impact of the elimination of Lat is different depending upon the stimulation state of cells and the specific phosphosite surveyed. Thus, Lat null cells show a mild increase in the phosphorylation of Vav1 in the entire molecule (Fig. 2B, compare 0 time points in upper panel) and in some tyrosine residues (Y^{142} and Y^{836}) (Fig. 2B, compare 0 time points in second and fifth panels from top, respectively) under nonstimulated conditions (see scheme in Fig. 2C). They also show severe defects in the effective phosphorylation on the Vav1 Y^{160} and Y^{174} (Fig. 2B, third and fourth panel from top, respectively) and, to a much lesser extent, the Y^{142} and Y^{836} (Fig. 2B, second and fifth panel from top, respectively) residues upon TCR stimulation (Fig. 2C). The right amount of immunoprecipitated Vav1 in all these samples was confirmed by the reblotting of the filters with antibodies to total Vav1 (Fig. 2B, three bottom panels). These results indicate that Lat has a major, although differential influence in the phosphorylation of the key regulatory Vav1 phosphosites. Consistent with these results, we found that Lat is essential for the proper stimulation of the Rac1-JNK axis by EGFP-$Vav1^{WT}$ in both nonstimulated and TCR-stimulated conditions (Fig. 2D). It also has some minor influence in the effector output of activated Vav1, as inferred by the reduced level of JNK activation induced by EGFP-$Vav1^{\Delta 1–186}$ when expressed in Lat-deficient cells (Fig. 2D, compare two upper graphs). These defects are similar to those previously seen in Lck-deficient cells (see above, Fig. 1D). JNK can be stimulated at similar levels in PMA-treated WT and ANJ3 cells (Fig. 2D, bottom panels), indicating that the foregoing defects are not due to the development of a spurious signaling deficiency in those mutant cells. Expression of the ectopic proteins in these experiments was confirmed by immunoblot analyses (Fig. 2E). These results indicate that Lat plays negative and positive roles in Vav1 phosphorylation in nonstimulated and stimulated cells, respectively (Fig. 2C). In addition, they further indicate the lack of a conserved pattern of phosphorylation dynamics for all the regulatory Vav1 phosphosites surveyed in this study.

2.2 Slp76 and PLCγ1 negatively regulate Vav1 phosphorylation

We next investigated the possible influence of the downstream Slp76 and PLCγ1 proteins on Vav1 phosphorylation. These two proteins participate in the Vav1 catalysis-independent pathway that leads to the stimulation of the transcriptional factor NFAT (Fig. 1B) and, in fact, can form signaling complexes with Vav1 during T cell signaling [30–32]. However, prima facie, they should not have any effect on the catalysis-dependent output of Vav1 (Fig. 1B). In contrast to this idea, we unexpectedly found using mutant Jurkat cells lacking either Slp76 (J14 clone, Fig. 3A) [33] or PLCγ1 (J.gamma1 clone, Fig. 3B) [34] that the elimination of any of these two signaling proteins results in high levels of basal phosphorylation of Vav1 in the absence of TCR stimulation (Fig. 3C, compare 0 time points). Upon TCR stimulation, Slp76- and PLCγ1-deficient cells both show delayed phosphorylation kinetics of Vav1 (Fig. 3C). Using Western blot analyses of total cell lysates, we observed that the deficiency of these two proteins only leads to increased phosphorylation in a limited number of signaling molecules (Fig. S2A, middle and left panels). Furthermore, we observed that the deficiency in Slp76 does not trigger elevated amounts of PLCγ1 phosphorylation in nonstimulated cells and, as expected [34], causes a defective phosphorylation of PLCγ1 in TCR-stimulated Jurkat cells (Fig. S4A). In line with this, we did not find any significant effect of the lack of PLCγ1 in the phosphorylation

levels of Slp76 in nonstimulated cells (Fig. S4B). Likewise, the elimination of Vav1 does not cause any significant increase in the phosphorylation of either Slp76 or PLCγ1 in Jurkat cells (Fig. S4C and S4D). Taken together, these results indicate that the increased phosphorylation of Vav1 in these two deficient cells is a specific event only shared by a very limited number of TCR downstream elements. Additional experiments indicated that the alteration in the steady state levels of Vav1 phosphorylation is probably mediated by a noncatalytic, adaptor-like function of PLCγ because: (i) We could not mimic the effect of the loss of PLCγ1 on Vav1 phosphorylation when using PLCγ (U73122) and protein kinase C (GF109203X) inhibitors in parental cells (Fig. S4E). As control, these inhibitors can eliminate the TCR-mediated phosphorylation of protein kinase D (PKD) (Fig. S4F), an enzyme known to be activated by the products of PLCγ1 enzyme activity [35,36]. (iii) We could not restore normal Vav1 phosphorylation levels in PLCγ1-deficient cells using combinations of a calcium ionophore (ionomycin) and a protein kinase C agonist (PMA) to bypass the lack of IP_3 and diacylglycerol production in those cells, respectively (Fig. S4G). We also investigated whether this phenotype could result from the loss of interactions with tyrosine phosphatases that can associate with Slp76 such as Shp1 (also known as Ptpn6) and Shp2 (also known as Ptpn11) [37,38]. However, we did not find any alteration in either the basal or TCR-induced phosphorylation of endogenous Vav1 in Shp1- (Fig. S4H) and Shp2-depleted (Fig. S4I) Jurkat cells. We obtained similar results when treating WT cells with a Shp family chemical inhibitor (NSC-87877; Fig. S4J).

The enhanced phosphorylation of Vav1 found in these conditions has a significant impact on the biological activity of the protein, as assessed by the higher levels of JNK activity triggered by EGFP-$Vav1^{WT}$ in nonstimulated Slp76- (Fig. 3D; compare red bars in upper and middle graphs) and PLCγ1-deficient (Fig. 3D; compare red bars in middle and bottom graphs) Jurkat cells when compared to controls. This effect is not observed in TCR-stimulated cells (Fig. 3D; compare blue bars in the three graphs), indicating that the levels of phosphorylation achieved under these conditions are sufficient to trigger the optimal stimulation of Vav1. Further linking this effect to phosphorylation events, we observed that the levels of stimulation of JNK by constitutively active $Vav1^{\Delta 1–186}$ are Slp76- and PLCγ-independent (Fig. 3D). The expression of the Vav1 proteins used in these experiments was controlled by immunoblot analyses (Fig. 3E). These results indicate that Slp76 and PLCγ1 work together to maintain Vav1 in a nonphosphorylated state under nonstimulated conditions (Fig. 3F, red lanes).

2.3 Mutations of Vav1 Ac phosphosites unveil new Vav1 functional states

The extensive number of Vav1 phosphosites involved in the stimulation of Vav1 led us to hypothesize that this protein might acquire different functionally competent states along the stimulation cycle of lymphocytes depending upon the number of phosphate acceptor sites targeted at a given time during cell stimulation [23]. To assess this idea, we decided to check the effect of both individual and compound (either Tyr to Phe or Tyr to Glu) mutations in Vav1 phosphosites involved in the activation step of Vav proteins (Fig. 1A) [23]. With this approach, we expected to “freeze” Vav1 in transitional states associated with each of the phosphorylation-dependent stimulation steps that could potentially affect the overall signaling output of the activated protein. To get a comprehensive idea of the contribution

of these “frozen states” in downstream signaling, we tested those mutants using biological readouts that measure both the catalysis-dependent (JNK) and catalysis-independent (NFAT) activity of Vav1 (Fig. 1B). As in the case of JNK, these experiments were done using a reporter plasmid containing the luciferase gene under the control of the minimal IL2 promoter and 3 NFAT binding sites [39]. When we tested single mutations affecting each of the three phosphosites located on the Vav1 Ac region (Fig. 1A) in JNK assays, we observed that the Y142F, Y142E, Y160F, and Y160E mutations induce minor, although statistically significant effects in the activity of Vav1 in the absence of TCR stimulation (Fig. 4A and B). By contrast, the Vav1 Y174F and, to a larger extent the Y174E mutation promote higher levels of JNK activity in both nonstimulated and stimulated cells (Fig. 4A and B). In fact, the activity of the Y174E mutant was similar to that elicited by the Vav1 protein that lacks the three Ac inhibitory phosphosites (Y^{142}, Y^{160}, Y^{174}) (Fig. 4A and B, see $Vav1^{Y3xF}$ protein) [14,21,23]. We obtained similar data when the single Ac phosphosite Vav1 mutants were tested in NFAT assays in Jurkat cells (Fig. 4C and D, upper panels). These experiments also revealed that the fold-change elicited by the Y174E and Y174F mutants is always significantly larger in NFAT than in JNK assays (e.g., compare results obtained with both the Y174F and Y174E mutants relative to the wild type counterpart in Figs. 4A and C), suggesting that the stimulation of the NFAT route requires lower signaling thresholds than the Rac1-JNK pathway.

We observed that the $Vav1^{Y3xF}$ mutant triggers levels of JNK activity that were comparable to those elicited by the $Vav1^{Y174E}$ mutant (Fig. 4A and D; Fig. 4E and F, upper panels) [14,21,23]. However, it always shows lower activity than the single Y174F and Y173E mutants when tested in NFAT experiments regardless of the stimulation state of cells (Fig. 4E and F, lower panels). We ruled out that this could derive from excessive Rac1 signaling, because Vav1 mutants with either similar (e.g., $Vav1^{Y174E}$) or constitutive (e.g., $Vav1^{\Delta 835–845}$) activities in JNK assays do not show that behavior (Fig. 4C) [23]. To get further insight into the inhibitory effect elicited by the Y3xF mutation in NFAT signaling, we next compared the effect induced by the combination of mutations in two Ac phosphosites (Y142F + Y174F, Y160F + Y174F) in the activity of Vav1 in this catalysis-independent pathway. We found that $Vav1^{Y142F+Y174F}$ and $Vav1^{Y160F+Y174F}$ exhibit activities similar to $Vav1^{Y174F}$ and $Vav1^{Y3xF}$ in both nonstimulated and TCR-stimulated Jurkat cells (Fig. 5A and B, upper panels). $Vav1^{Y160F+Y174E}$ and $Va\text{-}v1^{Y160E+Y174E}$ also show activities similar to the respective $Va\text{-}v1^{Y160F+Y174F}$counterparts (Fig. 5C and D), ruling out that this problem could be due to the nature of the different side chains present in the mutated residues. It is worth noting that the negative effect of the Y160F and Y160E mutations is only observed in the context of compound mutations with the Y174 residue, as demonstrated by the $Vav1^{WT}$-like activities displayed by the single $Vav1^{Y160F}$ (Figs. 4C and 5C) and $Vav1^{Y160E}$ (Fig. 4C) mutant proteins in the same biological readout. The activity of these mutant proteins is conserved when the NFAT assays are performed in both nonstimulated and B cell receptor-stimulated DT40 B cells (Figs. 4C and D, 5A and B, C and D; lower panels in each case). We and others have shown before that this chicken cell line, which only expresses Vav3 [40], offers an adequate experimental model to study the signaling properties of Vav family proteins [40–42]. This result indicates that the biological effects of the mutations tested here are not Jurkat cell specific. The foregoing Vav1 phosphosite

mutants also show similar activities when tested in either *VAV1*$^{-/-}$ Jurkat [43] or *Vav3*$^{-/-}$ DT40 [40] cells (data not shown), ruling out that some of these effects could be due to any interference of the ectopically expressed proteins on the endogenous Vav family counterparts. Taken together, these results suggest that the phosphorylated Y^{160} and Y^{174} residues cooperate in the opening of the molecule that favors the stimulation of the catalytic activity and, in addition, facilitate the formation of a conformational state essential for the optimal engagement of the NFAT pathway (Fig. 5E) (see Discussion).

2.4 The Y^{836} phosphosite affects the activation and signaling diversification of Vav1

The above observations led us to further explore the effect of mutations in the other key Vav1 regulatory phosphosite (Y^{836}) located in the CSH3 region (Fig. 1A). As previously described [23], the expression of Vav1 protein carrying a Y to F mutation in that residue promotes an increase in JNK (Fig. 6A and B, upper panels) and NFAT (Fig. 6A and B, lower panels) activities under both nonstimulated and TCR-stimulated conditions when expressed in Jurkat cells. Likewise, the combination the Y174F and the Y836F mutations promotes a synergistic effect, leading to the induction of very high levels of JNK stimulation when the compound mutant protein is expressed in Jurkat cells irrespectively of their stimulation state (Fig. 6A and B, upper panels) [23]. The activity of Vav1$^{Y174F+Y836F}$ is in fact very similar to those displayed by Vav1$^{\Delta 1–186}$ and Vav1$^{\Delta 835–845}$ in the same experimental system [23]. A synergistic effect of the double Y174F + Y836F mutation is also found when the activity of the protein is tested in NFAT assays (Fig. 6A and B, lower panels). However, this effect is lost when the Y836F and the Y3xF mutations are concurrently made, leading to the generation of a protein that exhibits Vav1^{Y3xF}-like NFAT activity (Fig. 6A and B, lower panels). These results further suggest that the concurrent mutation of the Y^{160} and Y^{174} phosphosites creates a conformation compatible with Vav1-Rac1-JNK but not Vav1-NFAT signaling. Additional experiments further suggest that this NFAT competent signaling state is also conditioned by the CSH3 domain, because a Vav1 protein bearing the Y836E mutation is totally inactive when tested in NFAT assays both in Jurkat (Fig. 6C and D, middle and upper panel, respectively) and DT40 (Fig. 6C and D, lower panels) cells. However, this protein can induce levels of JNK activation similar to those elicited by Vav1^{Y836F} (Fig. 6C, upper panel). The inhibitory effect of the Y836E mutation is quite prominent, since its combination with the Y174F mutation also reduces the high amounts of NFAT activity typically seen in the case of the single Vav1^{Y174F} and double Vav1$^{Y174F+Y836F}$ mutant proteins in both Jurkat (Fig. 6C, middle panel) and DT40 (Fig. 6C, lower panel) cells. This effect is unlikely to be due to structural problems induced by the Y836F mutation in the CSH3 domain, because Vav1 proteins carrying truncated versions of the CSH3 that do not allow normal folding (Δ835–845) are highly active when tested both in JNK and NFAT assays in Jurkat and DT40 cells [23]. These results suggest that the NFAT signaling competent state of Vav1 is influenced by structural constraints established around the Y^{160} + Y^{174} and Y^{836} phosphosites. By contrast, those restraints are not required to trigger the Vav1-dependent Rac1-JNK signaling axis (Fig. 6E and F).

3 Discussion

Despite the functional connection of Vav family proteins with tyrosine phosphorylation events, this key regulatory step still constitutes a black box from a mechanistic point of view. This problem is particularly acute in lymphocytes, since both the activation and downstream signaling of these proteins can be potentially influenced by a large number of PTKs, coreceptors, phosphatases, and adaptor molecules [1]. Using Vav1 as a model, we have seen here that this regulatory process is even more complex than previously anticipated in terms of phosphorylation dynamics, upstream kinases, and regulatory feedback mechanisms involved. In addition, our results suggest that phosphosites present in both the Ac- and CSH3 can influence both the activation and signaling diversification properties of the protein.

One of the main results of this work is the discovery that the phosphorylation status of Vav1 is subjected to several regulatory layers. Thus, we have found that Lck and the canonical Lck → Zap70 cascade regulated Vav1 phosphorylation using convergent but not lineal pathways. These two pathways cooperate in the generation of the optimal pool of phosphorylated Vav1 proteins and, in addition, differentially affect the kinetics of phosphorylation of the Y^{836} phosphosite. The key kinase in the overall process is Lck because, unlike the case of Zap70, it affects the stimulation of the Rac1-JNK pathway by both WT and fully deregulated Vav1 proteins. A nonconventional phosphorylation mechanism is also seen in nonstimulated cells, where the basal phosphorylated state is mainly Lck-dependent. Our results also indicate that other Src family kinases can collaborate less efficiently in the Lck-dependent phosphorylation steps. We also have observed that the phosphorylation of the different Vav1 phosphosites does not follow a common mechanism, an issue that was impossible to address up to now using standard immunoblot analyses with PTyr antibodies. In agreement with this, we observed that some Vav1 phosphosites are differentially targeted by Lck and Zap70 and, in addition, undergo different phosphorylation dynamics (changes in amplitude or kinetics of the phosphorylation response) depending upon the kinase deleted in cells. This is, to our knowledge, the first example in which dissociated patterns of phosphorylation of specific phosphosites are seen in the case of Vav1 and family counterparts.

Unexpectedly, we found that Slp76 and PLCγ1 participate in a safety control mechanism that maintains Vav1 in a low phosphorylated state in nonstimulated cells. This is mediated by an adaptor-like, phospholipase-independent function that regulates the phosphorylation status of Vav1. Lat marginally participates in this process, since its elimination promotes a slight increase in the phosphorylation of some Vav1 phosphosites in naïve cells. The nature of this negative regulatory step remains unclear. Our findings rule out the implication of Shp1 and Shp2, two protein tyrosine phosphatases that can associate with Slp76-PLCγ1 complexes in cells. We have not detected either any significant upregulation of Vav1 phosphorylation in nonstimulated cells upon the shRNA-mediated knockdown of all the cytoplasmic tyrosine phosphatases known to be expressed in Jurkat cells (Ptpn3, Ptpn4, Ptpn22; MB and XRB, unpublished data) [44], thus suggesting that this regulatory step is either phosphatase-independent or redundantly mediated by several phosphatases at the same time. Other alternative scenarios include the possibility that the Slp76-PLCγ1 complex restricts the interaction of Vav1 with upstream kinases either by the sequestration of Vav1 in

cytoplasmic complexes or by inducing changes in the subcellular localization of the kinases themselves. Consistent with this latter idea, a recent proteomics-based report published during the elaboration of this work has unveiled that PLCγ1 can differentially affect the spectrum of tyrosine phosphorylated proteins in Jurkat cells by inducing changes in the normal subcellular localization of Lck [45]. This event limits the phosphorylation levels of Zap70 and ITAMs while promotes the phosphorylation of other proteins such as the T cell specific adaptor (Tsad), Itk, Pyk2 and, in line with our study, Vav1 itself [45].

Given the multistep phosphorylation of Vav1, it is possible that this protein will show transient signaling states when switching between the nonphosphorylated and the fully phosphorylated condition. Consistent with this idea, we have observed different biological activities of Vav1 proteins with mutations in single phosphosites as well as synergistic effects when phosphosites in the Ac and CSH3 are concurrently mutated. However, we also found specific subsets of phosphosite mutants (Y160F + Y174F, Y160F + Y174E, Y3xF + Y386F, Y836E, Y174F + Y836E) that cannot properly engage the NFAT pathway despite displaying full functionally in the stimulation of the Rac1-JNK signaling axis (Fig. 6E and F). This branch-specific effect rules out any deleterious effect of these mutations in the overall structure of the protein. It is also unlikely that the effect of these mutations is mediated by the disruption of the interaction of a SH2 protein because, if that were the case, the Y836F and Y386E mutations had to elicit similar deleterious effects in the Vav1-mediated stimulation of the NFAT pathway. However, our results clearly show that this is not the case. An effect in trans of the mutations affecting the Y^{160} residue is also unlikely unless we assume that the two Y^{160} and Y^{174} phosphosites work together in the binding of a common protein partner. However, it is difficult to envision a scenario in which the binding of that putative effector would be preserved in the case of Vav1 proteins lacking each of those sites. Taken together, these data are compatible with a model in which these mutations disrupt a conformation of the active protein required for proper NFAT pathway engagement. Given the key role of the Vav1 CH domain in NFAT signaling [1,6,9,14,20,21], it is likely that these mutations directly or indirectly affect the positioning of the CH domain in the ‘open’ conformation of the tyrosine-phosphorylated protein. Alternatively, it is possible that these mutations could alter the interaction of Vav1 with either membrane microdomains or down-stream elements such as PLCγ1 in cells. This latter defect has been proposed in fact as an explanation for the lack of NFAT activity of Vav1 proteins lacking the CH [9], although this view is not shared by others [8,20]. These two models are not mutually exclusive. Regardless of the mechanism involved, an interesting ramification from our results is that the stimulation of the catalysis-dependent pathways is mechanistically simpler and less restrained than the NFAT route. This feature opens the way for the independent regulation of these two pathways under physiological conditions via regulatory mechanisms such as posttranslational modifications, binding of protein partners, and the intensity of the extracellular stimuli received by cells. Further work will address whether this possibility does occur in vivo and, if that were the case, the in cis and in trans regulatory mechanisms involved in the downstream diversification of Vav1 signals. It will be also interesting to elucidate the structure of the full-length inactive and active Vav1 to shed light on the conformations required for the regulation of the activation and effector cycles of this protein.

4 Materials and methods

4.1 Antibodies

The polyclonal antibody to the Vav1 DH domain (Ref. 302-5) was raised in rabbits using a maltose binding protein-Vav1 DH fusion protein previously purified from *Escherichia coli* according to standard techniques. Polyclonal antibodies to the indicated Vav1 phosphosites have been described before [21,23]. Other polyclonal antibodies used include those to Lck (Santa Cruz Biotechnology), GAPDH (Santa Cruz Biotechnology), PLCγ1 (Cell Signaling Technology), Slp76 (Cell Signaling Technology), p-PKD (Cell Signaling), p-Erk (Cell Signaling), Shp1 (Cell Signaling) and Shp2 (Abcam). Monoclonal antibodies utilized include those to phosphorylated tyrosine residues (Santa Cruz Biotechnology), EGFP (Covance), tubulin α (Santa Cruz Biotechnology), CD3 (UCHT1 clone, Merk Millipore), fluorescein-isothiocyanate-labeled CD45 (BD Biosciences), Zap70 (Upstate Biotechnology) and chicken IgM (Southern Biotech).

4.2 Expression vectors

Mammalian expression vectors encoding specific point mutants of Vav1 (Table S1) were generated using the QuickChange mutagenesis kit (Agilent Technologies) using the oligonucleotides described in Table S2. All mutant cDNAs were subjected to sequence analysis for verification. The WT and rest of Vav1 mutant proteins were previously generated in the laboratory [14,21,23,24]. The pNFAT-Luc plasmid was a gift from Dr. G. R. Crabtree (Howard Hughes Medical Institute, Stanford University, USA). The pFR-Luc and pFA2-cJun plasmids were purchased from Stratagene (now Agilent Technologies). The pRL-SV40 plasmid was from Promega.

4.3 Cell culture and treatments

WT, J.Cam1.6 [27] and J45.01 [28] Jurkat cells were purchased from the American Tissue Culture Collection. ANJ3 [29], P116 [26], J.gamma1 [34], and *VAV1*$^{-/-}$ [43] Jurkat cells were obtained from Drs. L.E. Samelson (Department of Cellular and Molecular Biology, Centre of Cancer Research, National Cancer Institute, Bethesda, MD, USA), B. Alarcón (Centro de Biología Molecular Severo Ochoa, CSIC, Madrid, Spain), A. Dunkan (Duke University, Durham, NC, USA), and R.T. Abraham (Duke University Medical Center, Durham, NC), respectively. J14 cells were previously described [33]. WT and *Vav3*$^{-/-}$ DT40 cells were obtained from the Riken Bioresource Center (Ibaraki, Japan) [40]. Jurkat cells were grown in RPMI-1640 supplemented with 10% fetal calf serum, 1% L-glutamine, penicillin (10 μg/ml) and streptomycin (100 μg/ml). DT40 cells were grown in RPMI-1640 medium supplemented with 10% fetal calf serum, 1% chicken serum, 0.1 mM β-mercaptoethanol, 1% L-glutamine, penicillin (10 μg/ml) and streptomycin (100 μg/ml). All cells were maintained in a humidified 5% CO_2 atmosphere at 37 °C.

Lymphoid cells were stimulated at 37 °C in serum free media by adding 10 μg/ml of antibodies to either CD3 (Jurkat cells) or chicken IgM (DT40 cells) for the indicated periods of time. In long-term stimulation experiments (Figs. 1D and 2D), Jurkat cells were also stimulated with PMA (50 ng/ml, Sigma Aldrich) and/or 1 μM ionomycin (Sigma-Aldrich) for 6 h in some cases. For short-term experiments (Fig. S4G), Jurkat cells were treated

with (1 μg/ml) and ionomycin (5 μg/ml, Sigma-Aldrich) for 2 h. Other treatments included the addition of 100 μM PP2 (Merck-Millipore, 1 h), 10 μM U73122 (Merck-Millipore, 30 min), 5 μM GF109203X (Sigma-Aldrich, 30 min) or NSC-87877 (25 and 50 μM; Merck-Millipore, 30 min) before the TCR stimulation step.

4.4 Immunoprecipitation and immunoblot analyses

Jurkat cells were lysed by adding 250 μl of an ice-cold buffer 5× lysis buffer (50 mM Tris-HCl [pH 7.5], 750 mM NaCl, 5% Triton X-100 [Sigma-Aldrich], 5 mM Na_3VO_4 [Sigma-Aldrich], 5 mM NaF [Sigma-Aldrich] and a mixture of protease inhibitors [Cømplete, Roche Life Science]) to 1 ml of cells in serum-free media. Upon centrifugation at 14,000 rpm for 10 min at 4 °C to eliminate cell debri, the lysates were incubated with 2 μl/ml of antibodies to the Vav1 DH domain and, subsequently, with Gammabind-Sepharose beads (GE Healthcare) for 120 and 45 min, respectively. When required, the immunoprecipitation state was carried out using antibodies to PLCγ1 and Slp76. Immunoprecipitates were washed three times with ice-cold 1× lysis buffer, boiled in sodium dodecyl sulfate-polyacrylamide gel electrophoresis sample buffer, separated electrophoretically in 8% denaturing gels, and transferred onto nitrocellulose filters using either a conventional liquid method (large gels) or an iBlot Dry Blotting System (Thermo Fisher Invitrogen, small gels) according to the supplier's protocol. For immunoblot analyses, nitrocellulose membranes were blocked in 5% bovine serum albumin (Sigma-Aldrich) in TBS-T (25 mM Tris-HCl (pH 8.0), 150 mM NaCl, 0.1% Tween-20) for 1 h, incubated with the indicated primary antibodies diluted in blocking solution for either 2 h (at room temperature) or overnight (at 4 °C). Membranes were then washed three times in TBS-T, incubated with either mouse or rabbit horseradish peroxidase-conjugated anti-IgG antibodies (GE Healthcare) in 5% non-fat dry milk in TBS-T for 45 min at room temperature (1:5000 dilution), washed three times in TBS-T, and finally subjected to a chemoluminiscence reaction (Thermo Fisher Pierce ECL system). When required, membranes were stripped with a diluted solution of Re-blot Plus Strong 10× (Merck-Millipore) for 15 min at room temperature and then reblotted as above. Total cellular lysates were extracted and analyzed by Western blot as above.

4.5 Biological assays

In the case of JNK activation assays using Vav1 proteins, Jurkat cells were electroporated (250 V and 950 μF) with pFA2-cJun (5 μg) and pFR-Luc (10 μg) together with control and experimental plasmids (20 μg each). After 36 h, cells were either left untreated or stimulated with 10 μg/ml of antibodies to CD3 and, 7 h later, lysed to record luciferase activities using the Dual Luciferase Reporter System according to the supplier's instructions (Promega). In the case of the stimulation of PMA and ionophore, cells were electroporated as above using the pFA2-cJun (5 μg), pFR-Luc (10 μg), and a vector constitutively expressing the *Renilla* luciferase (pRL-SV40; 5 ng). Cells were stimulated as indicated in previous sections for six hours. In the case of NFAT activation assays, exponentially growing Jurkat (2×10^7 cells) and DT40 cells (1×10^7) were electroporated as above with a luciferase reporter plasmid containing NFAT sites (pNF-AT/luc; 10 μg), pRL-SV40 (5 ng), and the appropriate experimental plasmids (20 μg). In all cases, electroporations were supplemented with empty plasmids to maintain a constant total amount of transfected DNA in all samples. Cells were either left untreated or stimulated with antibodies to CD3 (Jurkat cells) and IgM (DT40

cells), lysed and tested for luciferase activity as above. In this case, the values of firefly luciferase activity obtained in the different samples were normalized taking into account the activity of the *Renilla* luciferase obtained in each sample. Results presented in figures are given as the n-fold change observed in luciferase activity in a given sample relative to the values seen in nonstimulated, mock-electroporated cells (which were given an arbitrary value of 1). The abundance of the ectopic proteins was determined in all these experiments using immunoblot analyses of aliquots of the total cell lysates utilized in the luciferase determinations.

4.6 Generation of PTPN6 and PTPN11 knockdown Jurkat cells

To generate mRNA knockdowns in Jurkat cells, we used the Mission TRCN0000011052 and the Mission TRCN0000327984 lentivirus for eliminating the *PTPN6* and *PTPN11* transcripts, respectively. To this end, 20 μl of concentrated lentiviral supernatants were diluted in 2 ml of RPMI-1640 containing polybrene (8 μg/ml) and added onto 2×10^5 Jurkat cells plated in 6 well/plates. After centrifugation of the plates at 1500 rpm for 45 min at room temperature, the cells were cultured in the same plates overnight in a 37 °C incubator overnight under standard culture conditions. The transduction mix from each well was replaced the next morning by RPMI-1640 media supplemented with 10% fetal calf serum and, 48 h later, the cells were transferred into 75 mm^3 flasks for puromycin selection (1 μg/ml) for 5 days to generate the final knockdown pools. Effective knockdown in each case was verified using immunoblot analyses with the appropriate antibodies.

4.7 Image-processing

All images and figures were assembled and processed for final presentation using the Canvas Draw 2 for Mac software (ACD Systems).

4.8 Statistical analyses

The Mann-Whitney *U* test was applied to the data using three independent experiments, each performed in triplicate.

Supplementary Material

Refer to Web version on PubMed Central for supplementary material.

Acknowledgements

X.R.B. is supported by grants from the Castilla-León Government (BIO/SA01/15, CSI049U16), Spanish Ministry of Economy and Competitiveness (MINECO) (SAF2015-64556-R), Worldwide Cancer Research (14-1248), Ramón Areces Foundation, and Spanish Society against Cancer (GC16173472GARC). M.B. and S.R-F. salaries have been supported by a JAE-Predoc (CSIC) and MINECO FPI (BES-2013-063573) contracts for graduate students, respectively. Funding from MINECO is partially contributed by the European Regional Development Fund. The authors wish to thank M. Blázquez for technical assistance.

Data availability

No datasets have been generated in this work. All reagents generated by our lab for this work are freely available upon request.

References

[1]. Bustelo XR. Vav family exchange factors: an integrated regulatory and functional view. Small GTPases. 2014; 5 (2) 1–12.

[2]. Crespo P, Schuebel KE, Ostrom AA, Gutkind JS, Bustelo XR. Phosphotyrosine-dependent activation of Rac-1 GDP/GTP exchange by the vav proto-oncogene product. Nature. 1997; 385 (6612) 169–172. [PubMed: 8990121]

[3]. Bustelo XR. Vav proteins, adaptors and cell signaling. Oncogene. 2001; 20 (44) 6372–6381. [PubMed: 11607839]

[4]. Robles-Valero J, Lorenzo-Martin LF, Menacho-Marquez M, Fernandez-Pisonero I, Abad A, Camos M, Toribio ML, Espinosa L, Bigas A, Bustelo XR. A paradoxical tumor-suppressor role for the Rac1 exchange factor Vav1 in T cell acute lymphoblastic leukemia. Cancer Cell. 2017; 32 (5) 608–623. [PubMed: 29136506]

[5]. Robles-Valero J, Lorenzo-Martin LF, Fernandez-Pisonero I, Bustelo XR. Rho guanosine nucleotide exchange factors are not such bad guys after all in cancer. Small GTPases. 2018. 1–7.

[6]. Wu J, Katzav S, Weiss A. A functional T-cell receptor signaling pathway is required for p95vav activity. Mol Cell Biol. 1995; 15 (8) 4337–4346. [PubMed: 7623828]

[7]. Kuhne MR, Ku G, Weiss A. A guanine nucleotide exchange factor-independent function of Vav1 in transcriptional activation. J Biol Chem. 2000; 275 (3) 2185–2190. [PubMed: 10636924]

[8]. Zhou Z, Yin J, Dou Z, Tang J, Zhang C, Cao Y. The calponin homology domain of Vav1 associates with calmodulin and is prerequisite to T cell antigen receptor-induced calcium release in Jurkat T lymphocytes. J Biol Chem. 2007; 282 (32) 23737–23744. [PubMed: 17550897]

[9]. Knyazhitsky M, Moas E, Shaginov E, Luria A, Braiman A. Vav1 oncogenic mutation inhibits T cell receptor-induced calcium mobilization through inhibition of phospholipase Cgamma1 activation. J Biol Chem. 2012; 287 (23) 19725–19735. [PubMed: 22474331]

[10]. Macian F. NFAT proteins: key regulators of T-cell development and function. Nat Rev Immunol. 2005; 5 (6) 472–484. [PubMed: 15928679]

[11]. Aghazadeh B, Lowry WE, Huang XY, Rosen MK. Structural basis for relief of autoinhibition of the Dbl homology domain of proto-oncogene Vav by tyrosine phosphorylation. Cell. 2000; 102 (5) 625–633. [PubMed: 11007481]

[12]. Yu B, Martins IR, Li P, Amarasinghe GK, Umetani J, Fernandez-Zapico ME, Billadeau DD, Machius M, Tomchick DR, Rosen MK. Structural and energetic mechanisms of cooperative autoinhibition and activation of Vav1. Cell. 2010; 140 (2) 246–256. [PubMed: 20141838]

[13]. Movilla N, Bustelo XR. Biological and regulatory properties of Vav-3, a new member of the Vav family of oncoproteins. Mol Cell Biol. 1999; 19 (11) 7870–7885. [PubMed: 10523675]

[14]. Zugaza JL, Lopez-Lago MA, Caloca MJ, Dosil M, Movilla N, Bustelo XR. Structural determinants for the biological activity of Vav proteins. J Biol Chem. 2002; 277 (47) 45377–45392. [PubMed: 12228230]

[15]. Ksionda O, Saveliev A, Kochl R, Rapley J, Faroudi M, Smith-Garvin JE, Wulfing C, Rittinger K, Carter T, Tybulewicz VL. Mechanism and function of Vav1 localisation in TCR signalling. J Cell Sci. 2012; 125 (Pt 22) 5302–5314. [PubMed: 22956543]

[16]. Bustelo, XR, Dosil, M. Encyclopedia of Signaling Molecules. Choy, S, editor. Vol. 2018. Springer, Cham; New York: 5892–5906.

[17]. Bustelo XR. Regulatory and signaling properties of the Vav family. Mol Cell Biol. 2000; 20 (5) 1461–1477. [PubMed: 10669724]

[18]. Rapley J, Tybulewicz VL, Rittinger K. Crucial structural role for the PH and C1 domains of the Vav1 exchange factor. EMBO Rep. 2008; 9 (7) 655–661. [PubMed: 18511940]

[19]. Chrencik JE, Brooun A, Zhang H, Mathews II, Hura GL, Foster SA, Perry JJ, Streiff M, Ramage P, Widmer H, Bokoch GM, et al. J Mol Biol. 2008; 380 (5) 828–843. [PubMed: 18589439]

[20]. Li SY, Du MJ, Wan YJ, Lan B, Liu YH, Yang Y, Zhang CZ, Cao Y. The N-terminal 20-amino acid region of guanine nucleotide exchange factor Vav1 plays a distinguished role in T cell receptor-mediated calcium signaling. J Biol Chem. 2013; 288 (6) 3777–3785. [PubMed: 23271736]

[21]. Lopez-Lago M, Lee H, Cruz C, Movilla N, Bustelo XR. Tyrosine phosphorylation mediates both activation and downmodulation of the biological activity of Vav. Mol Cell Biol. 2000; 20 (5) 1678–1691. [PubMed: 10669745]

[22]. Robles-Valero J, Lorenzo-Martín LF, Menacho-Marquez M, Fernández-Pisonero I, Abad A, Camós M, Toribio ML, Espinosa L, Bigas A, Bustelo XR. A paradoxical tumor suppressor role for the Rac1 exchange factor Vav1 in T cell acute lymphoblastic leukemia. Cancer Cell. 2017; 32: 608–623. [PubMed: 29136506]

[23]. Barreira M, Fabbiano S, Couceiro JR, Torreira E, Martinez-Torrecuadrada JL, Montoya G, Llorca O, Bustelo XR. The C-terminal SH3 domain contributes to the intramolecular inhibition of Vav family proteins. Sci Signal. 2014; 7 (321) ra35 [PubMed: 24736456]

[24]. Schuebel KE, Movilla N, Rosa JL, Bustelo XR. Phosphorylation-dependent andconstitutive activation of rho proteins by wild-type and oncogenic Vav-2. EMBO J. 1998; 17 (22) 6608–6621. [PubMed: 9822605]

[25]. Chan AC, Desai DM, Weiss A. The role of protein tyrosine kinases and protein tyrosine phosphatases in T cell antigen receptor signal transduction. Annu Rev Immunol. 1994; 12: 555–592. [PubMed: 8011291]

[26]. Williams BL, Schreiber KL, Zhang W, Wange RL, Samelson LE, Leibson PJ, Abraham RT. Genetic evidence for differential coupling of Syk family kinases to the T-cell receptor: reconstitution studies in a ZAP-70-deficient Jurkat T-cell line. Mol Cell Biol. 1998; 18 (3) 1388–1399. [PubMed: 9488454]

[27]. Goldsmith MA, Weiss A. Isolation and characterization of a T-lymphocyte somatic mutant with altered signal transduction by the antigen receptor. Proc Natl Acad Sci U S A. 1987; 84 (19) 6879–6883. [PubMed: 3309950]

[28]. Koretzky GA, Picus J, Schultz T, Weiss A. Tyrosine phosphatase CD45 is required for T-cell antigen receptor and CD2-mediated activation of a protein tyrosine kinase and interleukin 2 production. Proc Natl Acad Sci U S A. 1991; 88 (6) 2037–2041. [PubMed: 1672451]

[29]. Zhang W, Irvin BJ, Trible RP, Abraham RT, Samelson LE. Functional analysis of LAT in TCR-mediated signaling pathways using a LAT-deficient Jurkat cell line. Int Immunol. 1999; 11 (6) 943–950. [PubMed: 10360968]

[30]. Wu J, Motto DG, Koretzky GA, Weiss A. Vav and SLP-76 interact and functionally cooperate in IL-2 gene activation. Immunity. 1996; 4 (6) 593–602. [PubMed: 8673706]

[31]. Tuosto L, Michel F, Acuto O. p95vav associates with tyrosine-phosphorylated SLP-76 in antigen-stimulated T cells. J Exp Med. 1996; 184 (3) 1161–1166. [PubMed: 9064333]

[32]. Fang N, Koretzky GA. SLP-76 and Vav function in separate, but overlapping pathways to augment interleukin-2 promoter activity. J Biol Chem. 1999; 274 (23) 16206–16212. [PubMed: 10347175]

[33]. Yablonski D, Kuhne MR, Kadlecek T, Weiss A. Uncoupling of nonreceptor tyrosine kinases from PLC-gamma1 in an SLP-76-deficient T cell. Science. 1998; 281 (5375) 413–416. [PubMed: 9665884]

[34]. Irvin BJ, Williams BL, Nilson AE, Maynor HO, Abraham RT. Pleiotropic contributions of phospholipase C-gamma1 (PLC-gamma1) to T-cell antigen receptor-mediated signaling: reconstitution studies of a PLC-gamma1-deficient Jurkat T-cell line. Mol Cell Biol. 2000; 20 (24) 9149–9161. [PubMed: 11094067]

[35]. Matthews SA, Rozengurt E, Cantrell D. Protein kinase D. A selective target for antigen receptors and a downstream target for protein kinase C in lymphocytes. J Exp Med. 2000; 191 (12) 2075–2082. [PubMed: 10859332]

[36]. Rozengurt E, Rey O, Waldron RT. Protein kinase D signaling. J Biol Chem. 2005; 280 (14) 13205–13208. [PubMed: 15701647]

[37]. Kwon J, Qu CK, Maeng JS, Falahati R, Lee C, Williams MS. Receptor-stimulated oxidation of SHP-2 promotes T-cell adhesion through SLP-76-ADAP. EMBO J. 2005; 24 (13) 2331–2341. [PubMed: 15933714]

[38]. Rhee I, Veillette A. Protein tyrosine phosphatases in lymphocyte activation and autoimmunity. Nat Immunol. 2012; 13 (5) 439–447. [PubMed: 22513334]

[39]. Clipstone NA, Crabtree GR. Identification of calcineurin as a key signalling enzyme in T-lymphocyte activation. Nature. 1992; 357 (6380) 695–697. [PubMed: 1377362]

[40]. Inabe K, Ishiai M, Scharenberg AM, Freshney N, Downward J, Kurosaki T. Vav3 modulates B cell receptor responses by regulating phosphoinositide 3-kinase activation. J Exp Med. 2002; 195 (2) 189–200. [PubMed: 11805146]

[41]. Caloca MJ, Zugaza JL, Matallanas D, Crespo P, Bustelo XR. Vav mediates Ras stimulation by direct activation of the GDP/GTP exchange factor Ras GRP1. EMBO J. 2003; 22 (13) 3326–3336. [PubMed: 12839994]

[42]. Caloca MJ, Zugaza JL, Bustelo XR. Mechanistic analysis of the amplification and diversification events induced by Vav proteins in B-lymphocytes. J Biol Chem. 2008; 283 (52) 36454–36464. [PubMed: 18974050]

[43]. Cao Y, Janssen EM, Duncan AW, Altman A, Billadeau DD, Abraham RT. Pleiotropic defects in TCR signaling in a Vav-1-null Jurkat T-cell line. EMBO J. 2002; 21 (18) 4809–4819. [PubMed: 12234921]

[44]. Gjorloff-Wingren A, Saxena M, Han S, Wang X, Alonso A, Renedo M, Oh P, Williams S, Schnitzer J, Mustelin T. Subcellular localization of intracellular protein tyrosine phosphatases in T cells. Eur J Immunol. 2000; 30 (8) 2412–2421. [PubMed: 10940933]

[45]. Belmont J, Gu T, Mudd A, Salomon AR. A PLC-gamma1 feedback pathway regulates Lck substrate phosphorylation at the T-cell receptor and SLP-76 complex. J Proteome Res. 2017; 16 (8) 2729–2742. [PubMed: 28644030]

Europe PMC Funders Author Manuscripts

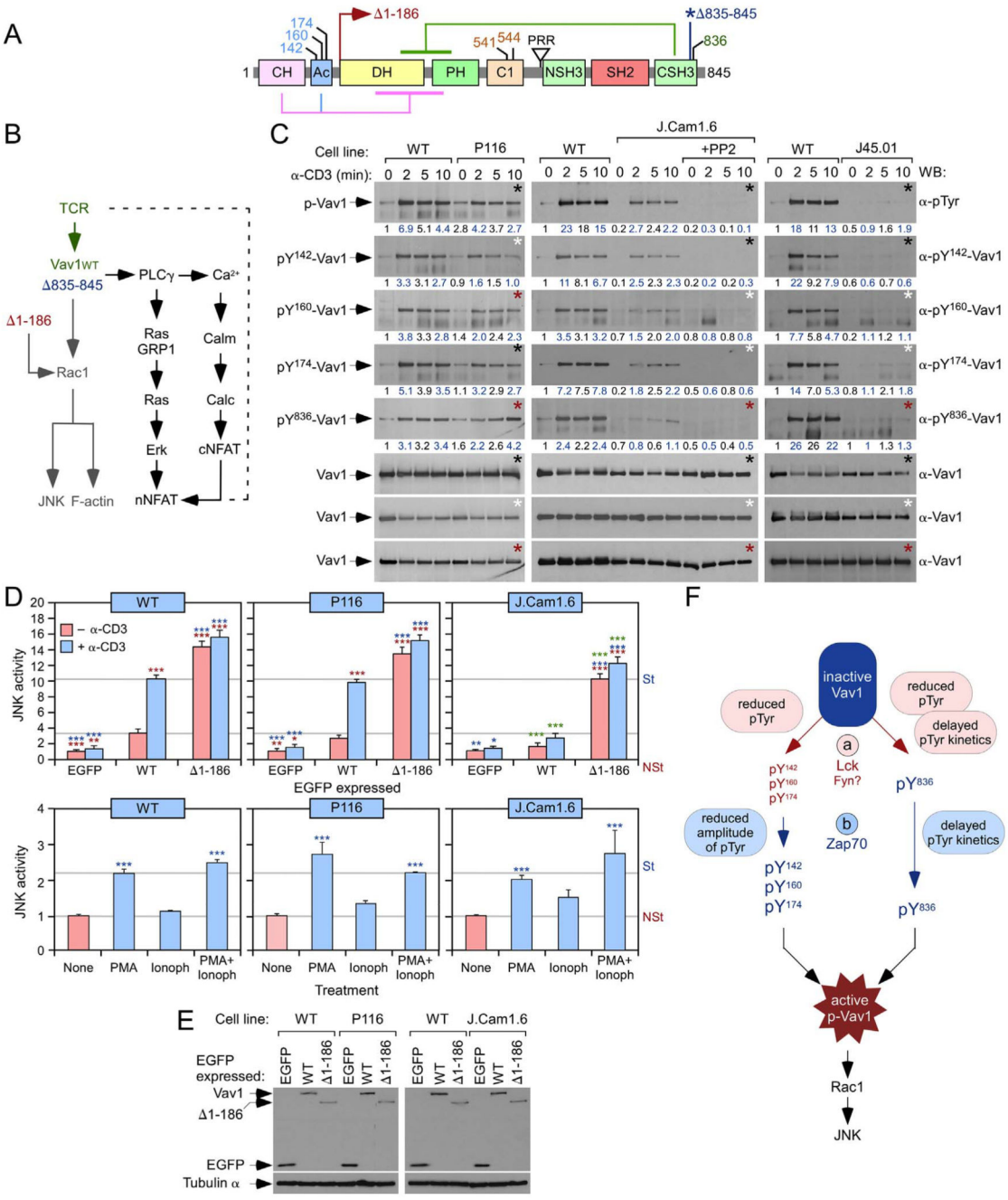

Fig. 1. Tyrosine kinases involved in the Vav1 phosphorylation step.

(A) Vav1 structure indicating phosphosites and intramolecular interactions contributing to Vav1 activity regulation. Phosphosites involved in each intramolecular interaction are depicted in the same color. The truncated N- (Δ1–186) and C-terminal (Δ835–845) mutants used in this study are also indicated.

(B) Simplified view of the Vav1-dependent Rac1-JNK (gray) and NFAT (black) pathways present in lymphocytes [3]. RasGRP1, Ras guanosine nucleotide releasing protein 1 (a

Europe PMC Funders Author Manuscripts

diacylglycerol regulated Ras GEF); Calm, calmodulin; Calc, calcineurin; cNFAT, cytosolic NFAT; nNFAT, nuclear NFAT.

(C) Vav1 immunoprecipitates from indicated cells and stimulation conditions were subjected to Western blot (WB) analyses with antibodies shown on the right. Filters were then stripped and reblotted with antibodies to Vav1 (the same filter is indicated with asterisks of the same colour). At the bottom of panels from phosphorylation detection, we present the densitometry values obtained for each immunoprecipitate (given an arbitrary value of 1 to the phosphorylation levels of Vav1 in nonstimulated WT cells). These values were normalized considering the total amount of immunoprecipitated Vav1 obtained in each sample. Please, note that the values can be only compared in each panel and not between panels (given that they were subjected to different exposure times). p-, phospho.

(D) *Top panels*, JNK activation levels in indicated EGFP-expressing Jurkat cell lines (top) that were either left nonstimulated (−) or stimulated (+) with antibodies to CD3. Values are shown as means ± SEM from four independent experiments, each performed in triplicate. *P* values are given relative to nonstimulated (red asterisks) and stimulated (blue asterisks) cells expressing EGFP-Vav1^{WT} in the same cell line. We also included *P* values for the values exhibited by each Vav1 protein relative to those obtained in WT cells (green asterisks). In this latter case, we have not included statistics in mock-transfected cells for the sake of simplicity. *, $P \leq 0.05$; **, $P \leq 0.01$; ***, $P \leq 0.001$. NSt, nonstimulated; St, stimulated. *Bottom panels*, JNK activation levels in indicated Jurkat cell lines (top) upon stimulation with the indicated compounds (bottom). Ionoph, ionophore. Values and *P* values are given as in top panels.

(E) Example of the abundance of ectopically expressed Vav1 obtained in one the experiments used for panel D.

(F) Summary of the results obtained in this figure. Lck- and Zap70-dependent steps are depicted in red and blue colour, respectively. The defects induced by the elimination of each kinase are boxed. (For interpretation of the references to colour in this figure legend, the reader is referred to the web version of this article.)

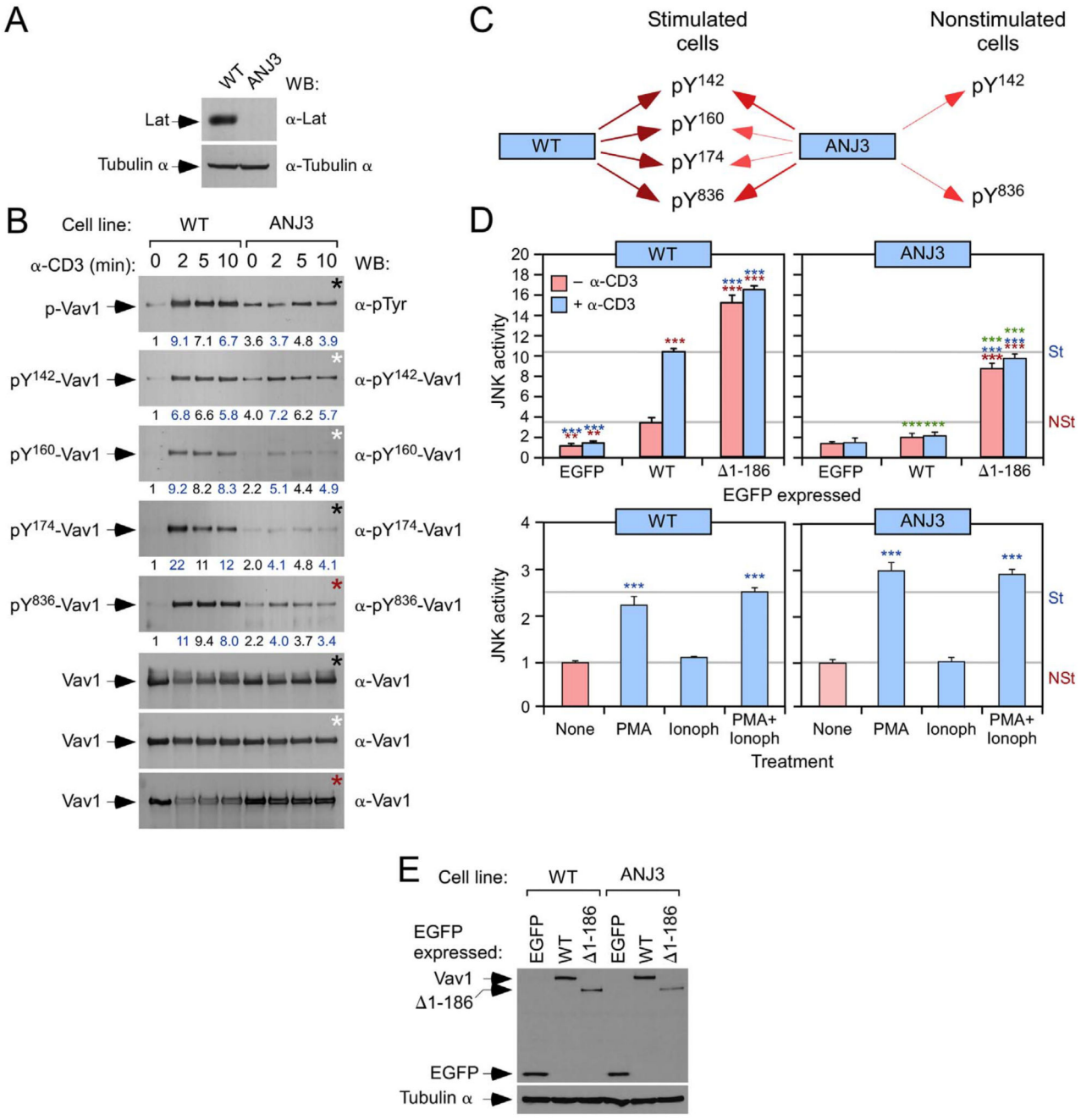

Fig. 2. Differential effect of Lat in the phosphorylation of Vav1 phosphosites.

(A) Immunoblots demonstrating the expected lack of expression of Lat in the ANJ3 Jurkat cell line.

(B) Vav1 immunoprecipitates from WT and ANJ3 Jurkat cells under the described stimulation conditions (top) were subjected to WB analyses with the indicated antibodies (right). The filters were then stripped and reblotted as indicated in Fig. 1C. At the bottom of each phosphorylation detection experiment, we present the normalized values of Vav1 phosphorylation calculated as indicated in Fig. 1C.

(C) Summary of the data obtained in B. Arrow thickness depicts the effect of the Lat deficiency in the phosphorylation of the indicated phosphosites under the described experimental conditions.
(D) JNK activation levels induced by either EGFP-Vav1^{WT} (top panels) or the indicated compounds (bottom panels) in WT and Lat-deficient Jurkat cells. In the case of the top panels, cells were stimulated with antibodies to CD3 as indicated. Experimental and statistical values are given as in Fig. 1D (n = 3, each performed in triplicate).
(E) Example of the abundance of ectopically expressed Vav1 obtained in one of the experiments made in panel D. (For interpretation of the references to colour in this figure legend, the reader is referred to the web version of this article.)

Europe PMC Funders Author Manuscripts

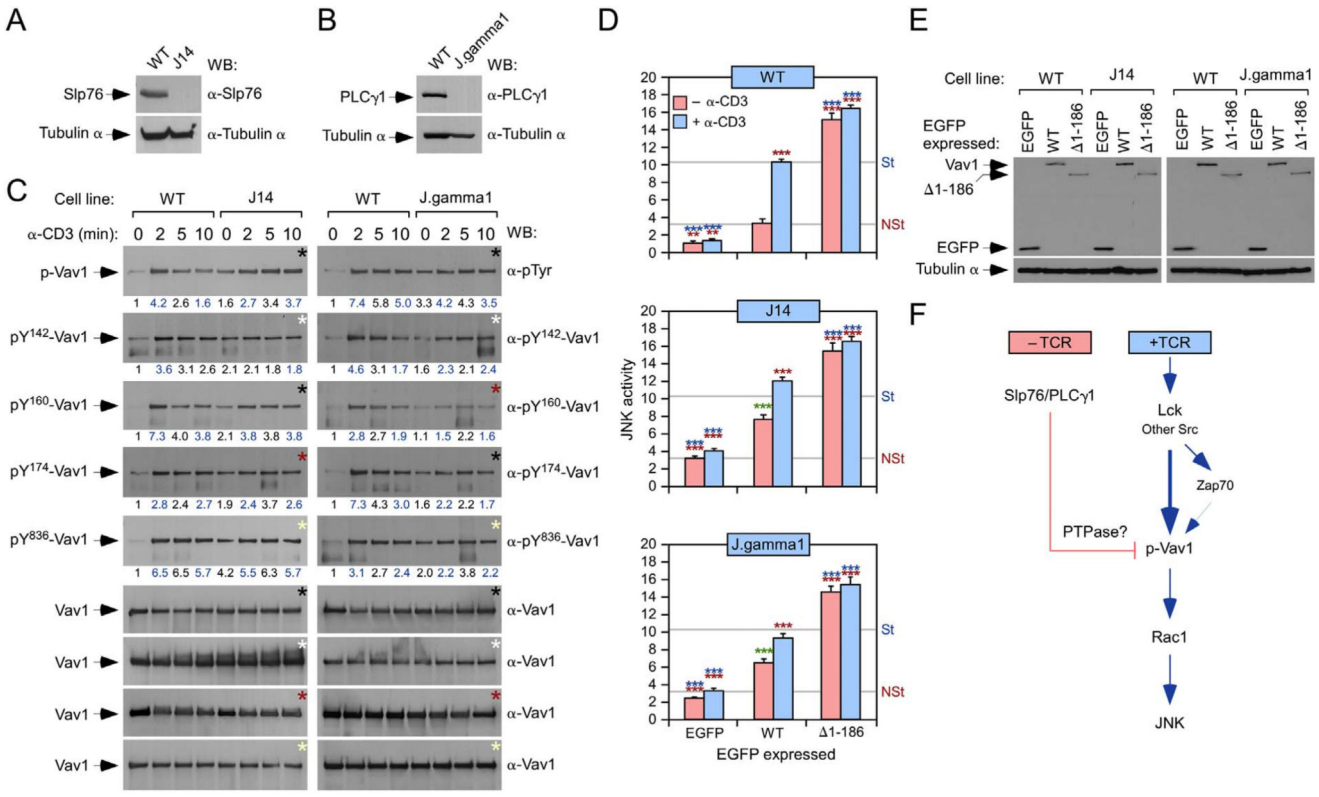

Fig. 3. Slp76 and PLCγ1 control the phosphorylation state of Vav1 in nonstimulated T cells.

(A and B) Immunoblots demonstrating the expected lack of expression of Slp76 (A) and PLCγ1 (B) in J14 and J.gamma1 Jurkat cells, respectively.

(C) Vav1 immunoprecipitates from WT, J14 and J.gamma1 cells under the described stimulation conditions (top) were subjected to WB analyses with indicated antibodies (right). Filters were then stripped and reblotted as indicated in Fig. 1C. At the bottom of each phosphorylation detection experiment, we present the normalized values of Vav1 phosphorylation calculated as indicated in Fig. 1C.

(D) JNK activity levels induced by indicated EGFPs in the described cells and stimulation conditions. Experimental and statistical values are given as in Fig. 1D ($n = 3$, each performed in triplicate).

(E) Example of the abundance of ectopically expressed Vav1 obtained in one of the experiments included in panel D.

(F) Summary of the results obtained in Figs. 1 and 3. Pathways present in nonstimulated (−TCR) and stimulated (+TCR) cells are shown in red and blue, respectively. Activation and inactivation steps are shown as arrows and blunted lanes, respectively. PTPase, potential tyrosine phosphatase involved in the Vav1 dephosphorylation step. (For interpretation of the references to colour in this figure legend, the reader is referred to the web version of this article.)

Europe PMC Funders Author Manuscripts

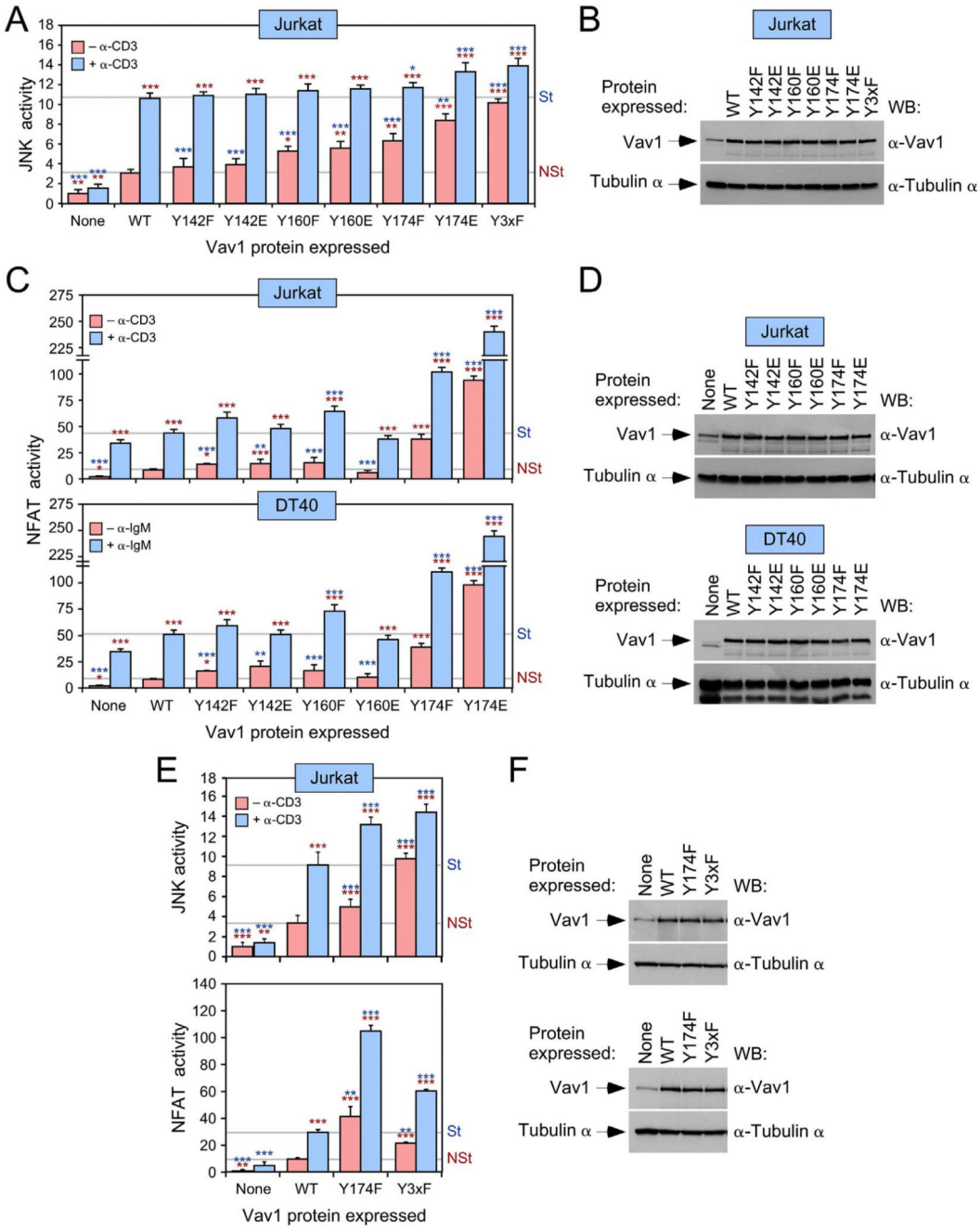

Fig. 4. Effect of mutations in Vav1 N-terminal phosphosites in downstream signaling.

(A) JNK activity levels induced by indicated Vav1 proteins in nonstimulated (−) and TCR-stimulated (+) Jurkat cells. Experimental and statistical values are given as in Fig. 1D ($n = 3$, each performed in triplicate).

(B) Example of the abundance of ectopically expressed Vav1 obtained in one of the experiments included in panel A.

Europe PMC Funders Author Manuscripts

(C) Stimulation of NFAT induced by indicated Vav1 proteins in nonstimulated (−) and receptor-stimulated (+) Jurkat (top) and DT40 (bottom) cells. Experimental and statistical values are given as in Fig. 1D ($n = 3$, each performed in triplicate).
(D) Example of the abundance of ectopically expressed Vav1 obtained in two of the experiments included in panel C.
(E) JNK (top panel) and NFAT (bottom panel) activity levels induced by indicated Vav1 proteins in nonstimulated (−) and TCR-stimulated (+) Jurkat cells. Experimental and statistical values are given as in Fig. 1D ($n = 3$, each performed in triplicate).
(F) Examples of the abundance of ectopically expressed Vav1 obtained in representative experiments performed in panel E.

Europe PMC Funders Author Manuscripts

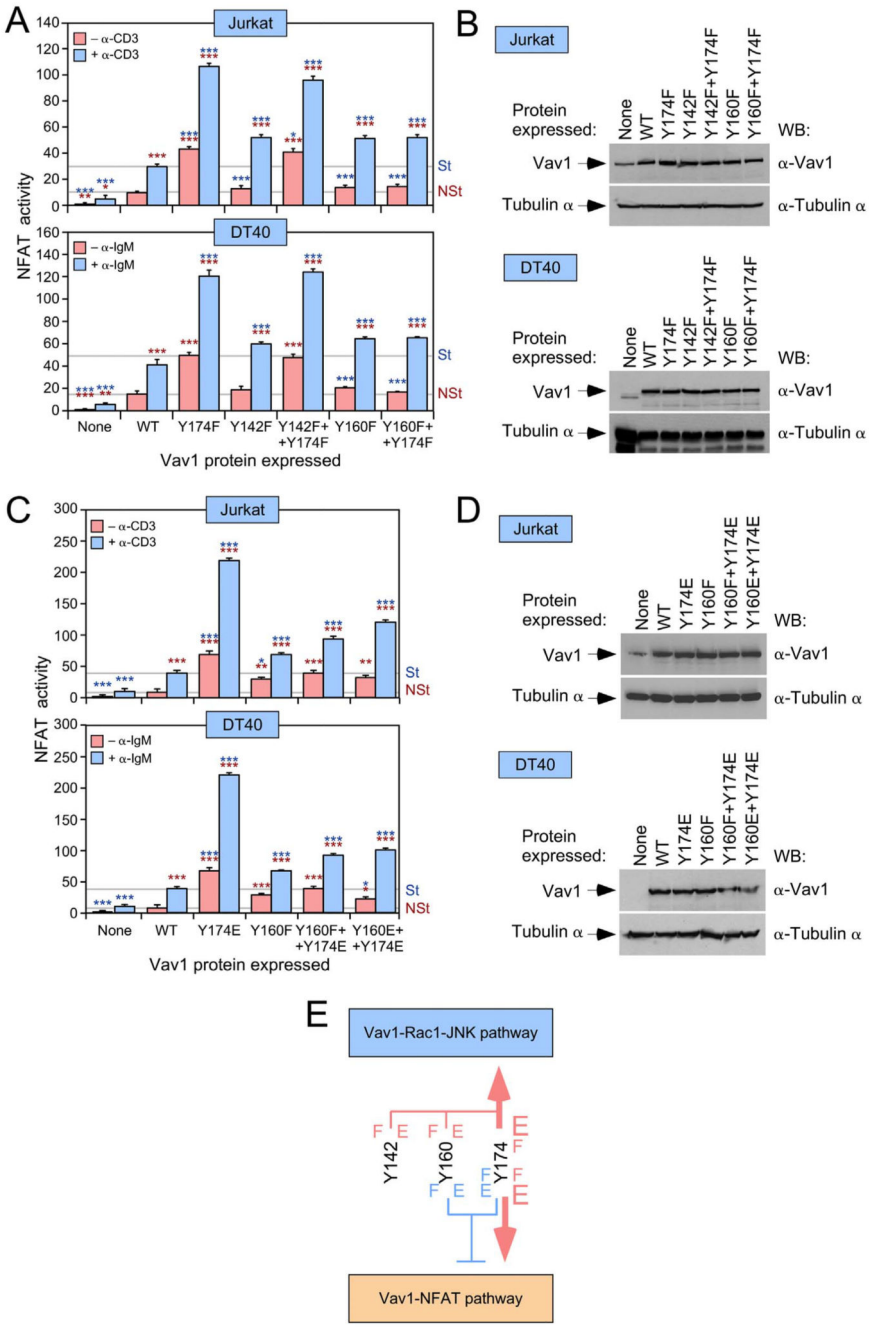

Fig. 5. Mutations of Vav1 Ac phosphosites unveil new Vav1 functional states.

(A) Stimulation of NFAT induced by indicated Vav1 proteins in nonstimulated (−) and receptor-stimulated (+) Jurkat (top) and DT40 (bottom) cells. Experimental and statistical values are given as in Fig. 1D ($n = 3$, each performed in triplicate).

(B) Examples of the abundance of ectopically expressed Vav1 in representative experiments performed in panel A.

Europe PMC Funders Author Manuscripts

(C) Stimulation of NFAT induced by indicated Vav1 proteins in nonstimulated (−) and receptor-stimulated (+) Jurkat (top panel) and DT40 (bottom panel) cells. Experimental and statistical values are given as in Fig. 1D ($n = 3$, each performed in triplicate).
(D) Examples of the abundance of ectopically expressed Vav1 obtained in representative experiments performed in panel C.
(E) Summary of the effect of indicated Vav1 mutations in the stimulation of the Rac1-JNK and NFAT pathways. Activation and inactivation steps are shown with red arrows and blue blunted lanes. F, Y to F mutation. E, Y to E mutation. The thickness of the lanes and the size of the letters represent the intensity of the effect induced. (For interpretation of the references to color in this figure legend, the reader is referred to the web version of this article.)

Europe PMC Funders Author Manuscripts

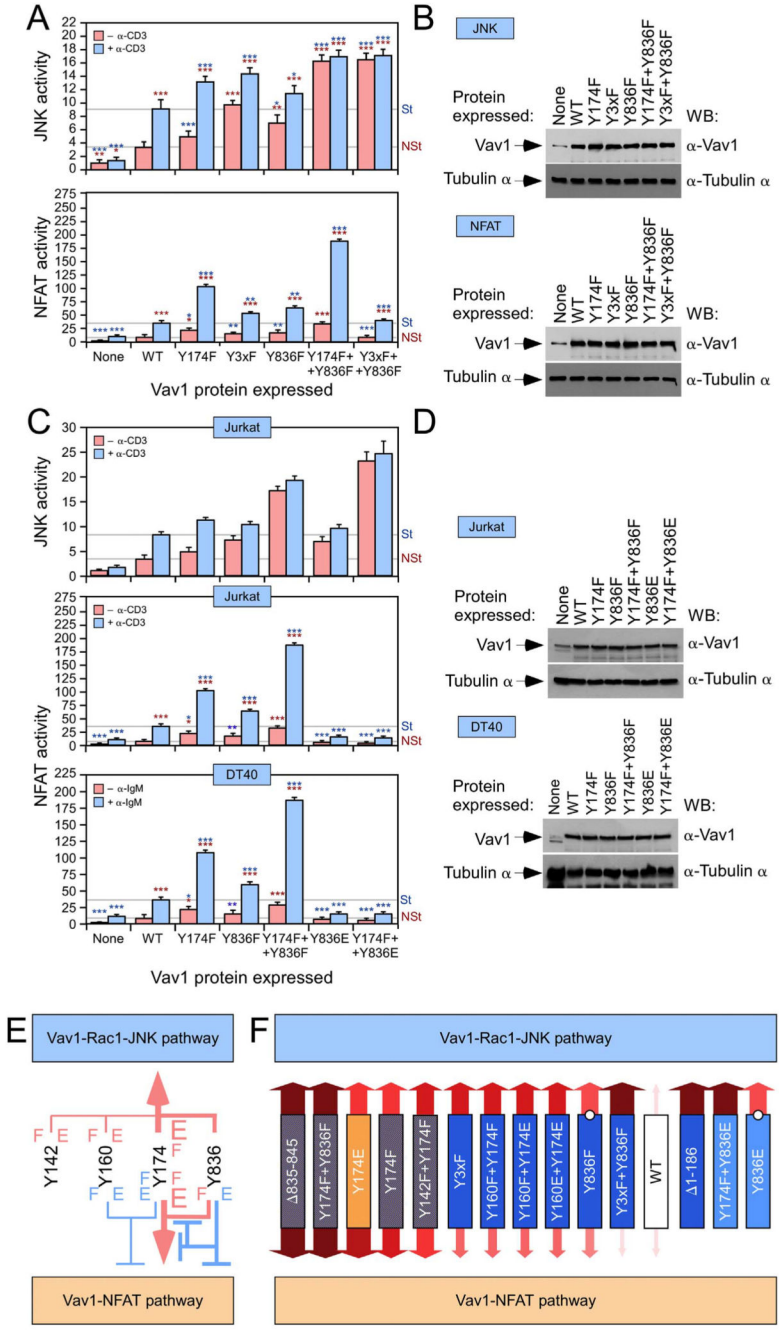

Fig. 6. The Y^{836} phosphosite affects the activation and signaling diversification of Vav1.

(A) JNK (top panel) and NFAT (bottom panel) activity levels induced by indicated Vav1 proteins in nonstimulated (−) and receptor-stimulated (+) Jurkat cells. Experimental and statistical values are given as in Fig. 1D (n = 3, each performed in triplicate).

(B) Examples of the abundance of ectopically expressed Vav1 obtained in representative experiments performed in panel A.

(C) JNK (upper panel) and NFAT (middle and lower panel) activity levels induced by indicated Vav1 proteins in nonstimulated (−) and receptor-stimulated (+) Jurkat (two top

panels) and DT40 (bottom panel) cells. Experimental and statistical values are given as in Fig. 1D ($n = 3$, each performed in triplicate).

(D) Examples of the abundance of ectopically expressed Vav1 obtained in representative experiments performed in panel C.

(E and F) Summary of the effect of indicated Vav1 mutations in the stimulation of the Rac1-JNK and NFAT pathways. In E, see legend to Fig. 5E for further details. In F, each mutation is included within a colored box that indicates the main effect in each respective pathway (blue, preferential effect in the Rac1-JNK route; brown, preferential effect in the NFAT pathway; mixed colors, similar effect in both pathways). The intensity of signal the output of each mutant is illustrated by the thickness and colour intensity of the arrows. The open circle indicates that the effect is only induced in nonstimulated cells. If not present, the effect is seen in both nonstimulated and stimulated cells. The results shown for $Vav1^{\Delta 1–186}$ and $Vav1^{\Delta 835–845}$ are based in previous publications [14,21,23]. (For interpretation of the references to color in this figure legend, the reader is referred to the web version of this article.)

Europe PMC Funders Author Manuscripts